Is It Possible to Synthesize a Low-Valent Transition Metal Complex with a Neutral Carbon Atom as Terminal Ligand? A Theoretical Study of $(CO)_4FeC$†

Yu Chen, Wolfgang Petz, and Gernot Frenking*

Fachbereich Chemie, Philipps-Universität Marburg, Hans-Meerwein-Strasse, D-35032 Marburg, Germany

Received March 22, 2000

Quantum chemical calculations at the NL-DFT (B3LYP) and CCSD(T) levels of theory have been carried out for the carbon complex $(CO)_4FeC$. The bonding situation was analyzed with the NBO partitioning scheme and with the topological analysis of the electron density distribution. The results have been compared with the bonding situations in $(CO)_4FeCH_2$, $I(CO)_3FeCH$, and $Fe(CO)_5$. The trigonal-bipyramidal complex $(CO)_4FeC$ with an axial Fe−C bond is a minimum on the singlet potential energy surface, while the equatorial form is a transition state. The Fe−C bond has a large dissociation energy, $D_e = 84.1$ kcal/mol at B3LYP/II and $D_e = 94.5$ kcal/mol at CCSD(T)/II. The carbon ligand is a strong π-acceptor and an even stronger σ-donor. The analysis of the electronic structure suggests that $(CO)_4FeC$ should behave like a carbon nucleophile. Geometry optimization of the donor−acceptor complex $(CO)_4FeC{-}BCl_3$ yielded a strongly bonded compound, which has a calculated C−B bond energy of $D_e = 25.6$ kcal/mol at B3LYP/II. Lewis acid stabilized carbon complexes such as $(CO)_4FeC{-}BCl_3$ might become isolated under appropriate conditions.

1. Introduction

Transition metal (TM) alkyl compounds which have a $TM{-}CR_3$ single bond have been known since 1848, when Frankland accidentally synthesized diethylzinc while he attempted to prepare a free ethyl radical.[1] Molecules with a $TM{=}CR_2$ double bond[2,3] and $TM{\equiv}CR$ triple bond[4,5] became isolated much later. TM carbene and carbyne complexes have been the focus of intensive experimental investigations since that time, because it was soon recognized that they are versatile compounds for organometallic synthesis.[6] The bonding situation in molecules with transition metal−carbon multiple bonds also attracted the interest of theoreticians, who were intrigued by the finding that there are two classes of carbene and carbyne complexes that exhibit different chemical behavior. The different reactivity was explained with a bonding model that suggests different metal−carbene[7] and metal−carbyne[8] interactions in the two classes of compounds. It was proposed that one class of compounds has donor−acceptor metal−carbon bonds, while the other class has normal (shared-electron) covalent bonds where the metal and the carbon atom each contribute one electron to a two-electron bond. This is schematically shown in Scheme 1. Very recent ab initio calculations proved that the bonding situations depicted in Scheme 1 are useful models for Fischer-type and Schrock-type carbene and carbyne complexes having donor−acceptor bonds or shared-electron interactions, respectively.[9] Because the metal−carbon bonds in Schrock-type compounds are not donor−acceptor bonds, they are better called alkylidenes and alkylidynes rather than carbene and carbyne complexes.

The next member in the series of metal−carbon bonds $TM{-}CR_3$, $TM{-}CR_2$, TM−CR is a bond with a terminal carbon atom TM−C. Transition metal carbide complexes are experimentally known, but all except one feature carbon atoms with at least two nearest neighbors.[10] The only example of a TM complex with a terminal carbon atom is the anion $(NRAr)_3MoC^-$, which is isoelectronic to the nitride complex $(NRAr)_3MoN$ ($R = C(CD_3)_2CH_3$, $Ar = C_6H_3Me_2$-3,5).[11] Scheme 1 also shows bonding models for a terminal TM−C donor−acceptor bond and a TM−C shared-electron bond which are similar to the

† Theoretical Studies of Organometallic Compounds. 40. Part 39: Beste, A.; Frenking, G. *Z. Anorg. Allg. Chem.* **2000**, *626*, 381.

(1) Elschenbroich, Ch.; Salzer, A. *Organometallics*, 2nd ed., VCH: Weinheim, 1992; p 1.

(2) Fischer, E. O.; Maasböl, A. *Angew. Chem.* **1964**, *76*, 645; *Angew. Chem., Int. Ed. Engl.* **1964**, *3*, 580.

(3) Schrock, R. R. *J. Am. Chem. Soc.* **1974**, *96*, 6796.

(4) Fischer, E. O.; Kreis, G.; Kreiter, C. G.; Müller, J.; Huttner, G.; Lorenz, H. *Angew. Chem.* **1973**, *85*, 618; *Angew. Chem., Int. Ed. Engl.* **1973**, *12*, 564.

(5) McLain, S. J.; Wood, C. D.; Messerle, L. W.; Schrock, R. R.; Hollander, F. J.; Youngs, W. J.; Churchill, M. R. *J. Am. Chem. Soc.* **1978**, *100*, 5962.

(6) (a) Dötz, K. H.; Fischer, H.; Hofmann, P.; Kreissl, F. R.; Schubert, U.; Weiss, K. *Transition Metal Carbene Complexes*; Verlag Chemie: Weinheim, 1983. (b) Dötz, K. H. *Pure Appl. Chem.* **1983**, *55*, 1689. (c) Dötz, K. H. *Angew. Chem.* **1984**, *96*, 573; *Angew. Chem., Int. Ed. Engl.* **1984**, *23*, 587. (d) Hegedus, L. S. *Pure Appl. Chem.* **1990**, *62*, 691. (e) Fischer, H.; Hofmann, P.; Kreissl, F. R.; Schrock, R. R.; Schubert, U.; Weiss, K. *Carbyne Complexes*; VCH: New York, 1988. (f) *Transition Metal Carbyne Complexes*; Kreissl, F. R., Ed.; Kluwer Academic Publishers: Dordrecht, The Netherlands, 1993. (g) Mayr, A.; Hoffmeister, H. *Adv. Organomet. Chem.* **1991**, *32*, 227. (h) Kim, H. P.; Angelici, R. J. *Adv. Organomet. Chem.* **1987**, *27*, 51. (i) Nugent, W. A.; Mayer, J. M. *Metal-Ligand Multiple Bonds*; Wiley: New York, 1988.

(7) (a) Taylor, T. E.; Hall, M. B. *J. Am. Chem. Soc.* **1984**, *106*, 1576. (b) Carter, E. A.; Goddard, W. A., III. *J. Am. Chem. Soc.* **1986**, *108*, 4746.

(8) Hofmann, P. In ref 6a, p 59f.

(9) (a) Vyboishchikov, S. F.; Frenking, G. *Chem. Eur. J.* **1998**, *4*, 1428. (b) Vyboishchikov, S. F.; Frenking, G. *Chem. Eur. J.* **1998**, *4*, 1439.

10.1021/om000250o CCC: $19.00
Publication on Web 06/03/2000

Scheme 1. Schematic Representation of the Orbital Interaction between a Transition Metal and (a) Carbene Ligand; (b) Carbyne Ligand; (c) Carbon Ligand[a]

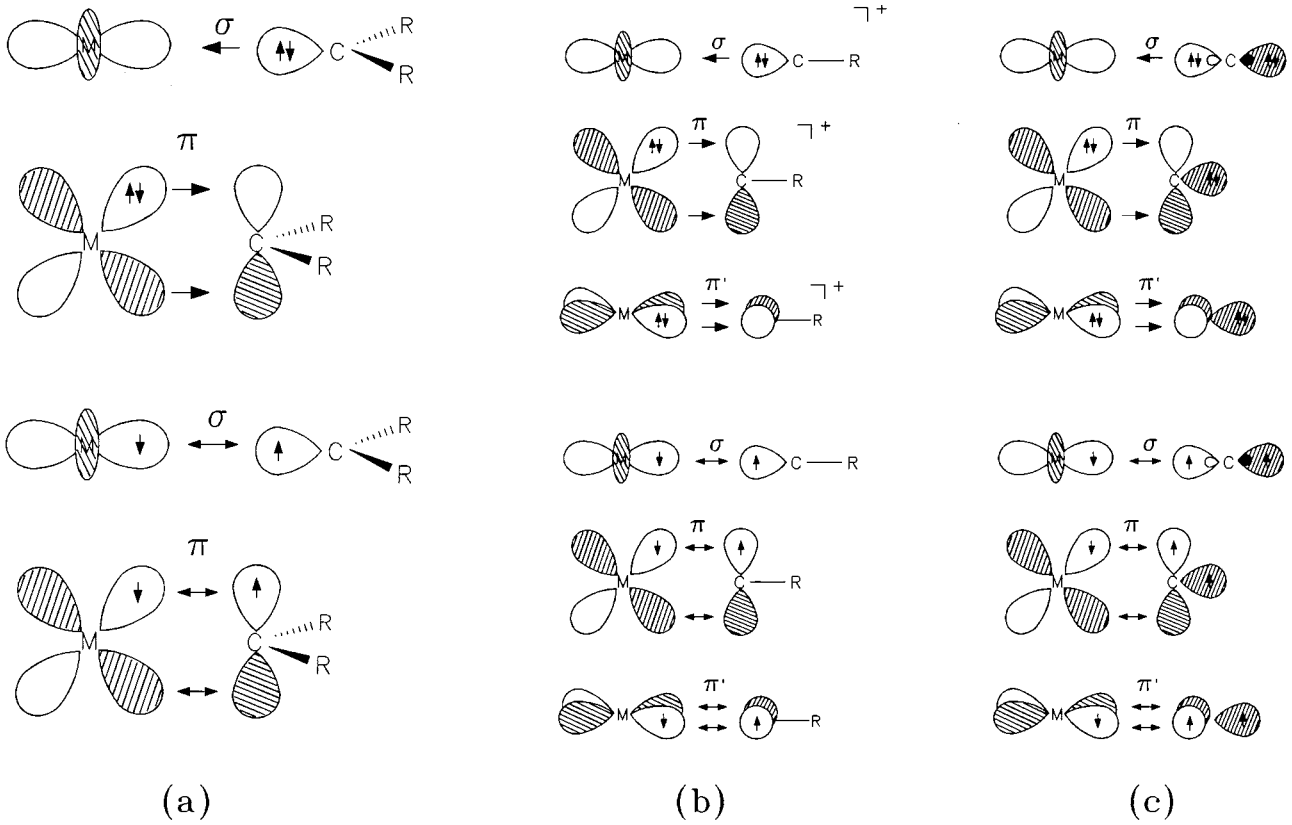

[a]Donor−acceptor interactions are shown on top; shared-electron bonding is shown on the bottom.

Scheme 2. Schematic Representation of the Electronic Configuration of Carbon in the ^1D State with and without Hybridization

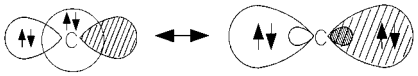

orbital models of the carbene and carbyne complexes. A carbon atom in the excited ^1D state (Scheme 2) has the same type of orbital interactions with a transition metal as a carbyne ligand (Scheme 1). An important difference is that the shared-electron TM−C bond leaves an unpaired electron at carbon, which explains why most TM carbides have carbon atoms with more than one nearest neighbor. In contrast to the shared-electron bond, the TM−C donor−acceptor bond has an electron lone pair at the terminal carbon atom. The bonding situation in negatively charged $(NRAr)_3MoC^-$ is analogous to $(NRAr)_3MoN$), which has a shared-electron Mo≡N triple bond and an electron lone pair. Thus, a complex with a transition metal−carbon donor−acceptor bond has not been synthesized so far. The carbon complex $(CO)_4FeC$ has been suggested as a possible intermediate in the reaction of $(CO)_4FeCS$ with $P(NMe_2)_3$.[12] We suggest that only compounds with a shared-electron TM−C bond should be called TM carbides, while those with a donor−acceptor bond are better called TM carbon complexes.[13]

In this paper we report about quantum chemical calculations of the model compound $(CO)_4FeC$ (**1**), which has an Fe−C donor−acceptor bond. We calculated the equilibrium geometry, Fe−C bond dissociation energy (BDE), and the vibrational frequencies of **1**. The nature of the chemical bond was analyzed with the help of the NBO[14] partitioning scheme and with the topological analysis of the electron density distribution.[15] For comparison, we also report about the bonding situation of $(CO)_4Fe(CH_2)$ (**2**), $I(CO)_3Fe(CH)$ (**3**), and $Fe(CO)_5$ (**4**). We are aware of the fact that **2** is not a good example of a stable Fischer-type carbene complex, because they can only become isolated when the carbene ligand has a π-donor substituent.[6a−d,i] The model compound **3** is a good reference species, however, for the discussion of the bonding situation and stability of **1**. The results of the calculations are used to predict the chemical properties of **1** and to discuss the possibilities to observe it

(10) (a) Chisholm, M. H.; Hammond, C. E.; Johnston, V. J.; Streib, W. E.; Huffman, J. C. *J. Am. Chem. Soc.* **1992**, *114*, 7056. (b) Caulton, K. G.; Cayton, R. H.; Chisholm, M. H.; Huffman, J. C.; Lobkovsky, E. B.; Xue; Z. *Organometallics* **1992**, *11*, 321. (c) Miller, R. L.; Wolczanski, P. T.; Rheingold, A. L. *J. Am. Chem. Soc.* **1993**, *115*, 10422. (d) Neithamer, D. R.; LaPointe, R. E.; Wheeler, R. A.; Richeson, D. S.; Van Duyne, G. D.; Wolczanski, P. T. *J. Am. Chem. Soc.* **1989**, *111*, 9056. (e) Mansuy, D.; Lecomte, J.-P.; Chottard, J.-C.; Bartoli, J.-F. *Inorg. Chem.* **1981**, *20*, 3119. (f) Goedkin, V. L.; Deakin, M. R.; Bottomley, L. A. *J. Chem. Soc., Chem. Commun.* **1982**, 607. (g) Latesky, S. L.; Selegue, J. P. *J. Am. Chem. Soc.* **1987**, *109*, 4731. (h) Etienne, M.; White, P. S.; Templeton, J. L. *J. Am. Chem. Soc.* **1991**, *113*, 2324.

(11) Peters, J. C.; Godom, A. L.; Cummins, C. C. *J. Chem. Soc., Chem. Commun.* **1997**, 1995.

(12) Petz, W.; Weller, F. *Organometallics* **1993**, *12*, 4056.

(13) Another bonding model for **1a** would be a shared-electron double bond between the unpaired electrons of triplet $Fe(CO)_4$ and the unpaired electrons of carbon in the triplet ground state. This leads to an iron atom in the formal oxidation state +2 and a carbon ligand with the formal charge −2, which is a rather unrealistic view.

(14) Reed, A. E.; Curtiss, L. A.; Weinhold, F. *Chem. Rev.* **1988**, *88*, 899.

(15) Bader, R. F. W. *Atoms in Molecules. A Quantum Theory*; Oxford Press: Oxford, 1990.

experimentally. To this end, we also calculated $(CO)_4FeC-BCl_3$ (**5**), which is a complex of the Lewis base **1** with the Lewis acid BCl_3.

2. Methods

The geometries have been optimized at the NL-DFT level using the three-parameter fit of the exchange−correlation potential suggested by Becke[16] in conjunction with the LYP[17] exchange potential (B3LYP).[18] A small-core ECP with a (441/2111/41) valence basis set for Fe,[19] an ECP with a (31/31/1) valence basis set for I,[20] and 6-31G(d) basis sets[21] for C, O, H have been employed in the geometry optimizations. This is our standard basis set II.[22] The nature of the stationary points was examined by calculating the Hessian matrix. Improved energy calculations at the B3LYP/II optimized geometries have been carried out using coupled-cluster theory[23] at the CCSD(T) level.[24] The calculations have been performed out with the program packages Gaussian 98,[25] ACES II,[26] and MOLPRO.[27]

3. Geometries, Bond Energies, and Vibrational Frequencies

Figure 1 shows the optimized geometries of **1**−**5** at B3LYP/II. Table 1 gives the calculated energies.

$(CO)_4FeC$ (**1a**) has a C_{3v} equilibrium geometry with an axial carbon ligand and a rather long $Fe-CO_{trans}$ bond. The isomeric form **1b**, which has the carbon ligand in the equatorial position, is a transition state on the potential energy surface. **1b** is calculated to be 7.7 kcal/mol higher in energy than **1a** (Table 1). The $(CO)_4Fe-C$ bond in **1a** is very short (1.614 Å). The $Fe-CO_{trans}$ bond of **1a** (2.052 Å) is much longer than the axial Fe−CO bonds in $Fe(CO)_5$ (**4**) (1.819 Å). The short $(CO)_4Fe-C$ bond and the lengthening of the $Fe-CO_{trans}$ bond with respect to **4** indicate that the Fe→C π-back-donation is quite strong, which concomitantly weakens the $Fe\rightarrow CO_{trans}$ back-donation.

The bonding model for the donor−acceptor bonds shown in Scheme 1 suggests that there are two Fe→C π-bonds in carbon complexes, while there is only one $Fe\rightarrow CR_2$ π-bond in carbene complexes. Figure 1 shows that the $Fe-CH_2$ bond in **2** is significantly longer than the Fe−C bond in **1a**. This holds for the isomer with the axial carbene ligand **2a** and for the equatorial isomer **2b**. In contrast to the carbon complex **1** we found that the equatorial form of the carbene complex **2b** is a minimum on the potential energy surface, while the axial form **2a** is a transition state which is 8.3 kcal/mol higher in energy than **2b** (Table 1). A previous qualitative analysis of the orbital interactions between $Fe(CO)_4$ and π-bearing ligands L led to the suggestion that π-acceptor ligands should prefer the equatorial position in $(CO)_4FeL$.[28] This is in agreement with the calculated equilibrium structure of **2b** and the experimental geometry of $(CO)_4Fe(C_2H_4)$.[29] The calculated energy minimum structure of $(CO)_4FeC$ (**1a**), however, defies the predicted preference of a π-acceptor ligand for an equatorial position.[28] A possible explanation for this is given in the section about the bonding situation.

Figure 1 shows also the calculated geometry of the carbyne complex $I(CO)_3Fe(CH)$ (**3**). The bonding model for the donor−acceptor bond of carbyne complexes L_n-TM−CR requires a somewhat arbitrary choice of charged fragments L_nTM^q and CR^q, because the neutral fragments are open-shell species. Scheme 1 exhibits the most common choice of a positively charged carbyne ligand and a negatively charged metal fragment. A recent theoretical analysis of the bonding situation in carbyne complexes has shown that this model is a reasonable qualitative representation of the TM−CR bond.[9b] Thus, the bonding situation in TM carbon and carbyne complexes should be quite similar. There are two metal−ligand π bonds, but according to the model, the π-back-donation in carbyne complexes should be stronger than in carbon complexes because the carbyne ligand CR has formally a positive charge. Figure 1 shows that the $I(CO)_3Fe-CH$ bond of **3** is indeed slightly shorter (1.601 Å) than the $(CO)_4Fe-C$ bond of **1a**. This lends some support to the bonding model for carbyne complexes (Scheme 1). It will be shown below, however, that the shorter Fe−CH bond is better explained with the hybridization of the σ-donor orbital of the CH ligand. We want to point out that the calculated bond lengths of $Fe(CO)_5$ (**4**) are in excellent agreement with the most recent experimental values (Fe−CO(ax) = 1.811(2) Å; Fe−CO(eq) = 1.803(2) Å).[30]

The analysis of the bonding situation that is given below suggests that the carbon ligand of **1** should exhibit nucleophilic rather than electrophilic behavior and that **1** can be classified as a Lewis base. We calculated the adduct of **1** with BCl_3. Figure 1 shows the equilibrium geometry of **5**, which is a minimum on the potential energy surface. The B−C donor−acceptor bond of **5** is very short (1.587 Å). It is significantly shorter than the

(16) Becke, A. D. *J. Chem. Phys.* **1993**, *98*, 5648.
(17) Lee, C.; Yang, W.; Parr, R. G. *Phys. Rev.* **1988**, *B37*, 785.
(18) Stevens, P. J.; Devlin, F. J.; Chablowski, C. F.; Frisch, M. J. *J. Phys. Chem.* **1994**, *98*, 11623.
(19) Hay, P. J.; Wadt, W. R. *J. Chem. Phys.* **1985**, *82*, 299.
(20) Bergner, A.; Dolg, M.; Küchle, W.; Stoll, H.; Preuss, H. *Mol. Phys.* **1993**, *80*, 1431.
(21) (a) Ditchfield, R.; Hehre, W. J.; Pople, J. A. *J. Chem. Phys.* **1971**, *54*, 724. (b) Hehre, W. J.; Ditchfield, R.; Pople, J. A. *J. Chem. Phys.* **1972**, *56*, 2257.
(22) Frenking, G.; Antes, I.; Böhme, M.; Dapprich, S.; Ehlers, A. W.; Jonas, V.; Neuhaus, A.; Otto, M.; Stegmann, R.; Veldkamp, A.; Vyboishchikov, S. F. *Reviews in Computational Chemistry*, Vol. 8; Lipkowitz, K. B., Boyd, D. B., Eds.; VCH: New York, 1996; pp 63−144.
(23) Cizek, J. *J. Chem. Phys.* **1966,** *45*, 4256.
(24) Pople, J. A.; Krishnan, R.; Schlegel, H. B.; Binkley, J. S. *Int. J. Quantum Chem.* **1978**, *14*, 545. Bartlett, R. J.; Purvis, G. D. *Int. J. Quantum Chem.* **1978**, *14*, 561. Purvis, G. D.; Bartlett, R. J. *J. Chem. Phys.* **1982**, *76*, 1910. Purvis, G. D.; Bartlett, R. J. *J. Chem. Phys.* **1987**, *86*, 7041. Pople, J. A.; Head-Gordon, M.; Raghavachari, K. *J. Chem. Phys.* **1987**, *87*, 5968.
(25) Frisch, M. J.; Trucks, G. W.; Schlegel, H. B.; Scuseria, G. E.; Robb, M. A.; Cheeseman, J. R.; Zakrzewski, V. G.; Montgomery, J. A.; Stratmann, R. E.; Burant, J. C.; Dapprich. S.; Milliam, J. M.; Daniels, A. D.; Kudin, K. N.; Strain, M. C.; Farkas, O.; Tomasi, J.; Barone, V.; Cossi, M.; Cammi, R.; Mennucci, B.; Pomelli, C.; Adamo, C.; Clifford, S.; Ochterski, J.; Petersson, G. A.; Ayala, P. Y.; Cui, Q.; Morokuma, K.; Malick, D. K.; Rabuck, A. D.; Raghavachari, K.; Foresman, J. B.; Cioslowski, J.; Ortiz, J. V.; Stefanov, B. B.; Liu, G.; Liashenko, A.; Piskorz, P.; Komaromi, I.; Gomberts, R.; Martin, R. L.; Fox, D. J.; Keith, T. A.; Al-Laham, M. A.; Peng, C. Y.; Nanayakkara, A.; Gonzalez, C.; Challacombe, M.; Gill, P. M. W.; Johnson, B. G.; Chen, W.; Wong, M. W.; Andres, J. L.; Head-Gordon, M.; Replogle, E. S.; Pople, J. A. *Gaussian 98* (Revision A.1); Gaussian Inc.: Pittsburgh, PA, 1998.
(26) Stanton, J. F.; Gauss, J.; Watts, J. D.; Lauderdale, W. J.; Bartlett, R. J. *ACES II*, an ab initio program system; University of Florida: Gainesville, FL, 1991.
(27) Werner, H.-J.; Knowles, P. J. *Users's Manual for MOLPRO*; University of Sussex, Sussex, UK, 1991.
(28) Albright, T. A.; Burdett, J. K.; Whangbo, M. H. *Orbital Interactions in Chemistry*; Wiley: New York, 1985; pp 320−325.
(29) Drouin, B. J.; Kukolich, S. G. *J. Am. Chem. Soc.* **1999**, *121*, 4023.
(30) Braga, D.; Grepioni F.; Orpen, A. G. *Organometallics* **1993**, *12*, 1481.

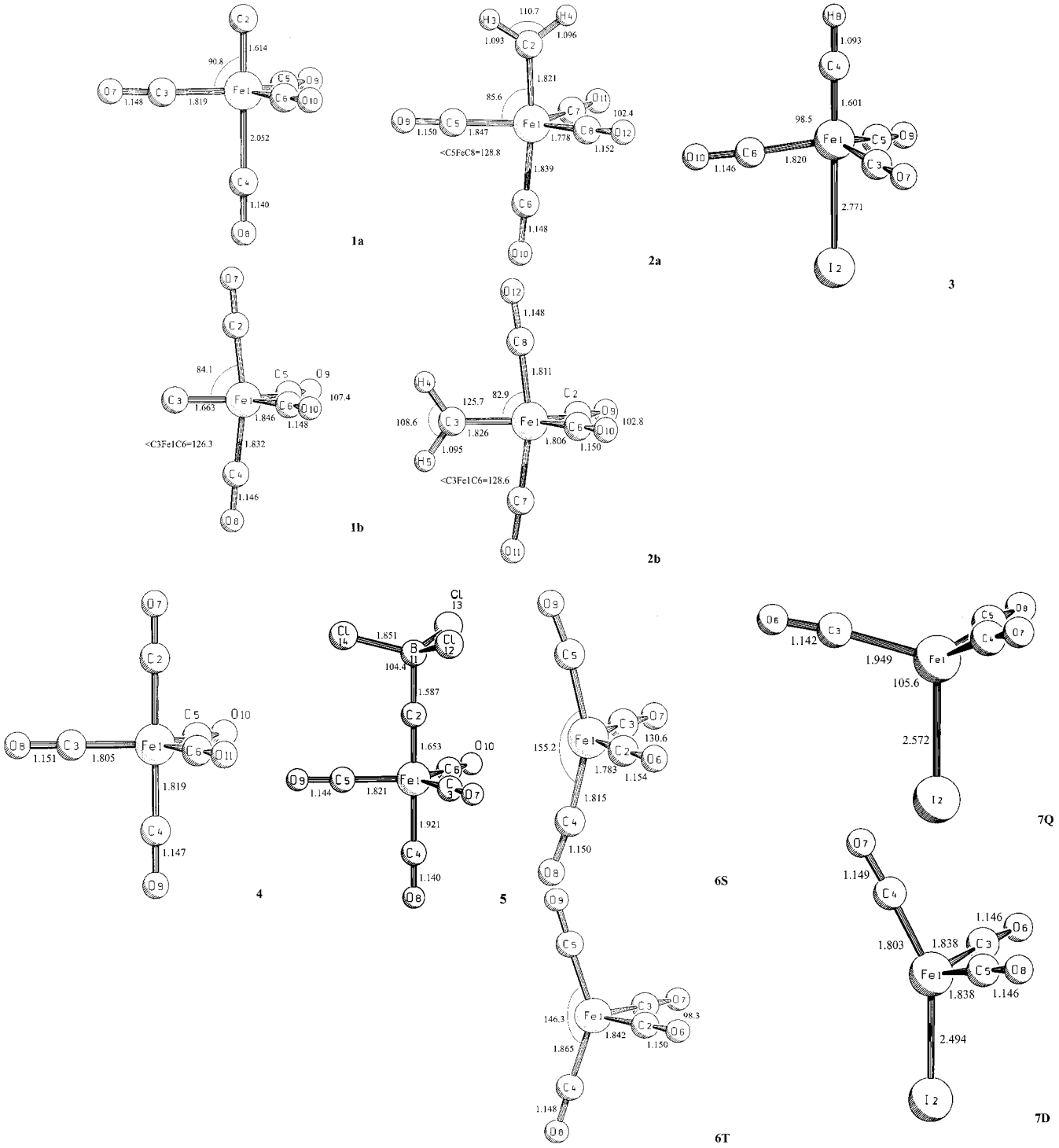

Figure 1. Optimized geometries (B3LYP/II) of **1**−**7**. Distances in Å, angles in deg.

theoretically predicted donor−acceptor bond of the diaminocarbene complex with boron trichloride $(NH_2)_2C-BCl_3$ (1.637 Å).[31] The iron−carbon bond of **5** is clearly longer (1.654 Å) than in the parent compound **1a**, and the $Fe-CO_{trans}$ bond of **5** becomes much shorter (1.918 Å), which indicates that the trans influence of the carbon ligand becomes weaker when it is bonded to a Lewis acid.

Figure 1 also gives the geometries of $Fe(CO)_4$ in the ($^1A_1$) singlet (**6S**) and ($^3B_2$) triplet (**6T**) states. The triplet form **6T** is predicted at the B3LYP/II level to be 8.3 kcal/mol lower in energy than **6S**. This is in agreement with previous calculations. Li et al.[32] calculated at the NL-DFT level a value of 1.7 kcal/mol in favor of the triplet state. Barnes et al.[33] carried out MCPF calculations of **6S** and **6T**. They estimated that the triplet state of $Fe(CO)_4$ should be 15 ± 5 kcal/mol below the singlet state. Thus, the calculated value of 8.3 kcal/mol seems to be reasonable. Unfortunately, the CCSD(T) calculation of

(31) Beste, A.; Krämer, O.; Gerhard, A.; Frenking, G. *Eur. J. Inorg. Chem.* **1999**, 2037.

(32) Li, J.; Schreckenbach, G.; Ziegler, T. *J. Am. Chem. Soc.* **1995**, *117*, 486.

(33) Barnes, L. A.; Rosi, M.; Bauschlicher, C. W., Jr. *J. Chem. Phys.* **1991**, *94*, 2031.

Table 1. Calculated Total Energies E_{tot} (au), Relative Energies E_{rel} (kcal/mol), Zero-Point Vibrational Energies ZPE (kcal/mol), and Number of Imaginary Frequencies *i*

			B3LYP/II/B3LYP/II				CCSD(T)/II/B3LYP/II	
molecule	no.	sym	E_{tot}	E_{rel}	ZPE	*i*	E_{tot}	E_{rel}
$(CO)_4FeC(ax)$	**1a**	C_{3v}	−614.77478	0.0	22.3	0	−612.94108	0.0
$(CO)_4FeC(eq)$	**1b**	C_{2v}	−614.76291	+7.5	22.7	1	−612.92881	+7.7
$(CO)_4FeCH_2(ax)$	**2a**	C_s	−616.05043	0.0	36.8	1	−614.18216	0.0
$(CO)_4FeCH_2(eq)$	**2b**	C_{2v}	−616.06076	−6.5	37.3	0	−614.19544	−8.3
$I(CO)_3FeCH$	**3**	C_{3v}	−513.51971		24.9	0	−511.82174	
$Fe(CO)_5$	**4**	D_{3h}	−690.15655		26.7	0	−688.13539	
$(CO)_4FeCBCl_3$	**5**	C_{3v}	−2020.36785		28.8	0	−2016.76742	
$Fe(CO)_4$ ($^1A_1$)	**6S**	C_{2v}	−576.78295	0.0	20.7	0	−575.02548	
$Fe(CO)_4$ ($^3B_2$)	**6T**	C_{2v}	−576.79610	−8.3	20.0	0	n.c.[a]	
$I(CO)_3Fe$ ($^4\Sigma$)	**7Q**	C_{3v}	−474.91911	0.0	14.4	0	n.c.[a]	
$I(CO)_3Fe$ ($^2\Pi$)	**7D**	C_1	−474.91299	3.8	15.7	0	n.c.[a]	
CO		$C_{\infty v}$	−113.30691		3.2	0	−113.03352	
CH_2 ($^3B_1$)		C_{2v}	−39.14912	0.0	10.9	0	−39.02160	0.0
CH_2 ($^1A_1$)		C_{2v}	−39.12705	+13.8	10.9	0	−38.99670	+15.6
CH ($^2\Pi$)		$C_{\infty v}$	−38.47770	0.0	4.0	0	−38.36240	0.0
CH ($^4\Sigma^-$)		$C_{\infty v}$	−38.44530	+20.2	4.4	0	−38.34544	+10.6
C (^3P)			−37.84469			0	−37.75180	
BCl_3		D_{3h}	−1405.55234		4.8	0	−1403.78278	

[a] Not converged.

Table 2. Calculated Bond Dissociation Energies D_e[a] and Metal−Ligand Interaction Energies E_{int}[b] (kcal/mol) (ZPE-Corrected Energies Are Given in Parentheses)

		B3LYP/II		CCSD(T)/II[c,e]	
molecule	no.	D_e (D_0)	E_{int}	D_e (D_0)	E_{int}
$(CO)_4Fe-C(ax)$	**1a**	84.1(81.8)	121.4(119.8)[d]	94.5(92.9)	131.9(130.3)[d]
$(CO)_4Fe-CH_2(eq)$	**2b**	72.5(66.1)	94.6(88.4)	84.8(79.1)	108.7(103.0)
$I(CO)_3Fe-CH$	**3**	76.4(70.2)			
$(CO)_4Fe-CO$	**4**	33.6(30.1)	41.8(39.0)	39.6(36.8)	47.9(45.1)
$(CO)_4FeC-BCl_3$	**5**	25.6(23.9)	25.6(23.9)	27.3(25.7)	27.3(25.7)

[a] Calculated with respect to the fragments in the electronic ground state. [b] Calculated with respect to the fragments in the lowest singlet state. [c] Using the B3LYP/II value of the singlet−triplet energy difference for $Fe(CO)_4$ (8.3 kcal/mol). [d] Calculated using the experimental value for the $^3P \rightarrow {}^1S$ excitation energy for carbon (29.1 kcal/mol). [e] Using the B3LYP/II optimized geometries.

6T did not converge. A triplet ground state of $Fe(CO)_4$ has also been deduced from experimental studies by analysis of MCD measurements.[34] The open-shell ($^4\Sigma$) state **7Q** of $I(CO)_3Fe$ is predicted at B3LYP/II to be 3.8 kcal/mol lower in energy than the ($^2\Pi$) state **7D**.

Table 2 gives the theoretically predicted bond dissociation energies D_e and donor−acceptor interaction energies E_{int} of **1**−**5**. The D_e values and the ZPE corrected D_o data of the iron−ligand bonds have been calculated for the dissociation of the Fe−L complexes yielding $Fe(CO)_4$ or $I(CO)_3Fe$ and L in the electronic ground states. The interaction energies E_{int} have been calculated with respect to the lowest lying singlet states of the metal fragment and L, which are relevant for the bonding models shown in Scheme 1. We do not give E_{int} values for the $I(CO)_3Fe-CH$ bond of **3**, because the dissociation of **3** into closed-shell fragments yields charged species. The associated dissociation energy thus involves a charge separation reaction, which should not be compared with the E_{int} values of **1a**, **2b**, and **4**. The D_e and E_{int} values of **5** are the same because the fragments of the bond dissociation reaction have singlet ground states.

The theoretically predicted $(CO)_4Fe-C$ bond dissociation energy of **1a** is very high. The calculated value at B3LYP/II is D_e = 84.1 kcal/mol. The CCSD(T)/II value D_e = 92.8 kcal/mol is even higher. The CCSD(T)/II values for the bond energies of **1**−**5** are always higher than the B3LYP/II results but not very much. The carbon complex **1a** has clearly the strongest metal−ligand bond of the investigated compounds. The carbyne complex **3** (D_e = 76.4 kcal/mol at B3LYP/II) and the carbene complex **2b** (D_e = 72.5 kcal/mol at B3LYP/II; D_e = 83.1 kcal/mol at CCSD(T)/II) also have strong Fe−L bonds, while $Fe(CO)_5$ (**4**) (D_e = 33.6 kcal/mol at B3LYP/II; D_e = 37.9 kcal/mol at CCSD(T)/II) is clearly weaker bonded. The latter values may be compared with the experimental value for the first bond dissociation energy of $Fe(CO)_5$ at 0 K, $D_o = 39 \pm 2$ kcal/mol.[35] However, this value refers to the dissociation of $Fe(CO)_5$ yielding the singlet state **6S** of $Fe(CO)_4$ and CO and, thus, must be compared with the ZPE-corrected E_{int} data given in Table 2. The theoretical values (38.3 kcal/mol at B3LYP/II; 42.7 kcal/mol at CCSD(T)/II) are in very good agreement with experiment.

The calculations predict that the order of the Fe−L bond dissociation energies D_e has the trend C > CH > $CH_2 \gg$ CO. A comparison with the optimized geometries shows that the Fe−L bond energies clearly do not correlate with the bond lengths. The $(CO)_4Fe-CO$ bond of **4** is shorter but significantly weaker than the $(CO)_4Fe-CH_2$ bond of **2b**, and the $(CO)_4Fe-C$ of **1a** is longer, but has a higher BDE than the $I(CO)_3Fe-CH$ bond of **3**. An explanation for the trend of the bond energies and for the bond length/bond energy correlation is given below in the section about bonding analysis.

We investigated the thermodynamic stabilization of the carbon ligand of **1a** by the $Fe(CO)_4$ fragment. The latter moiety is isolobal to CH_2.[36] Thus, $(CO)_4FeC$ may

(34) Poliakoff, M.; Weitz, E. *Acc. Chem. Res.* **1987**, *20*, 408.

(35) Lewis, K. E.; Golden, D. M.; Smith, G. P. *J. Am. Chem. Soc.* **1984**, *106*, 3905.

be compared with vinylidene H_2CC. We calculated the reaction energies of the hydrogenation of **1a** and vinylidene:

$$(CO)_4FeC\ (\mathbf{1a}) + H_2 \rightarrow (CO)_4FeCH_2\ (\mathbf{2b}) \quad (1)$$

$$H_2CC + H_2 \rightarrow H_2CCH_2 \quad (2)$$

The reaction energy for reaction 1 is predicted at B3LYP/II to be −69.3 kcal/mol (−80.1 kcal/mol at CCSD(T)/II). The theoretically predicted energy for reaction 2 is −95.6 kcal/mol (−107.5 kcal/mol at CCSD(T)/II). Thus, the $Fe(CO)_4$ fragment stabilizes a carbon atom 26.3 kcal/mol (B3LYP/II; 27.0 kcal/mol at CCSD(T)/II) more than methylene.

The interaction energies E_{int} involve the excitation energy of $Fe(CO)_4$ from the triplet ground state to the singlet excited state and the triplet→singlet excitation energies of C (in the case of **1**) and CH_2 (in the case of **2**). The first excited singlet state of carbon, which is relevant to the bonding model shown in Scheme 1, is the ^1D state, which cannot accurately be calculated at the single-determinant level.[37] We took the calculated energy of the ^3P ground state and the experimental value (29.1 kcal/mol)[38] for the $^3P \rightarrow {}^1D$ excitation energy in order to estimate E_{int} for **1a**. Table 2 shows that the E_{int} values discriminate the ligands C, CH_2, and CO even more than the D_e data. $(CO)_4Fe-C$ (**1a**) has a particularly large interaction energy, which correlates well with the short bond.

The calculated BDE of the $(CO)_4FeC-BCl_3$ bond (D_e = 25.6 kcal/mol at B3LYP/II; 27.3 kcal/mol at CCSD(T)/II) is large enough to make **5** a possible target for synthetic work.[43] It is interesting to compare the BDE of **5** with the calculated bond energy of the carbene complex $(NH_2)_2C-BCl_3$, which is D_e = 59.7 kcal/mol.[31] Thus, the latter carbene complex has a much stronger yet longer $C-BCl_3$ bond than **5**. It will be shown below that this can be explained with the hybridization at the carbon donor atom. The BDE of the $C-BCl_3$ bond of **5** is much higher, however, than the bond energy of $OC-BCl_3$ (D_e = 2.3 kcal/mol).[31] The rotation of the BCl_3 ligand of **5** around the Fe−C−B axis is nearly unhindered. The rotational barrier is only 0.2 kcal/mol (B3LYP/II).

Table 3 shows the theoretically predicted vibrational spectra of $(CO)_4FeC$ (**1a**) and $(CO)_4FeC-BCl_3$ (**5**), which might help to identify the compound. The calculated wavenumbers and IR intensities of **2**−**4** are given as Supporting Information. The Fe−C stretching mode of **1a** is predicted at ν = 969 cm^{-1}, but the IR intensity is very low. It could only be observed in the Raman spectrum. The Fe−C stretching mode in **5**, which is coupled to the B−C fundamental, is shifted to lower wavenumbers at ν = 700 cm^{-1}. It now has a high IR intensity and should help to identify the molecule. Also the B−C stretching mode at ν = 1128 cm^{-1} might be useful for this purpose.

Table 3. Calculated Vibrational Frequencies (cm^{-1}) and IR Intensities (km mol^{-1}) at B3LYP/II of $(CO)_4FeC$(ax) and $(CO)_4FeCBCl_3$

$(CO)_4FeC$(ax) (**1a**)				$(CO)_4FeCBCl_3$ (**5**)			
sym	mode	freq	(int)	sym	mode	freq	(int)
A_1	[CO]	2185	(226)	A_1	[CO]	2203	(484)
	[CO]	2151	(207)		[CO]	2172	(228)
	$[FeC]_{carbon}$	969	(1)		[BC]	1128	(122)
	[δFeCO]	535	(36)		$[BC]+[FeC]_B$	705	(282)
	$[FeC]_{eq}$	419	(0)		[δFeCO]	550	(46)
	$[FeC]_{ax}$	227	(8)		$[FeC]_{eq}$	419	(1)
	[δFeCO]	112	(0)		$[BCl]+[FeC]_{ax}$	391	(0)
A_2	[δFeCO]	368	(0)		$[FeC]_{ax}$	359	(12)
E	[CO]	2116	(1043)		[δCBCl]	186	(20)
	[δFeCO]	573	(86)		[δCFeC]	107	(1)
	[δFeCO]	475	(2)		[δFeCO]	369	(0)
	[δFeCO]	468	(0)		[δ(BCl_3C)-Fe(CO)]	3	(0)
	[δFeCO]	343	(0)		[CO]	2150	(836)
	[δCFeC]	185	(4)		[δFeCB]	720	(76)
	[δFeCO]	86	(0)		[δCFeC]	642	(157)
	[δCFeC]	54	(0)		[δFeCO]	521	(1)
					[δFeCO]	467	(3)
					[δFeCO]	406	(4)
					[δFeCO]	346	(0)
					[δClBCl]	223	(0)
					[δCFeC]	103	(0)
					[δCFeC]	93	(0)
					[δCFeC]	64	(0)
					[δCFeC]	31	(0)

4. Analysis of the Bonding Situation

We first discuss the NBO results shown in Table 4, which give insight into the Fe−L σ- and π-bonds of **1a**−**5**. The NBO method suggests for **1a** a Lewis structure which has a $(CO)_4Fe-C$ σ- and a degenerate π-bond. The σ- and the π-bonds are strongly polarized toward the iron atom. This holds particularly for the degenerate π-bond, which has a weight of 81.5% at the iron side. The polarization of the Fe−C σ-bond of **1a** is noteworthy, because it is the only one of the complexes **1a**−**5** that has a larger amplitude on the iron side, while the other σ-bonds are more polarized toward carbon. This indicates that the carbon ligand is a strong σ-donor in **1a**.

The carbon complex **1a** possesses the strongest polarized Fe−L bonds of the complexes **1a**−**5**. Another extreme value of **1a** is the hybridization of the σ bond at the carbon ligand. The NBO has mainly p character at carbon and only 14.4% s contribution. This is in strong contrast to the hybridization at the carbon atom of the CO ligand in $Fe(CO)_5$, which has 63.7% s character in the Fe−CO bond. The hybridization at carbon is one reason the $(CO)_4Fe-CO$ bond of **4** is comparatively short and yet significantly weaker than the Fe−L bonds of **1a**−**5**. The high percentage s character of the CO donor orbital means that it is rather compact and that the σ-orbital interactions take only place at shorter distances compared with donor orbitals

(36) Hoffmann, R. *Angew. Chem.* **1982**, *94*, 725; *Angew. Chem., Int. Ed. Engl.* **1982**, *21*, 711.

(37) The calculated $^3P \rightarrow {}^1D$ excitation energy at B3LYP/II (44.1 kcal/mol) and CCSD(T)/II (37.1 kcal/mol) is too high because of the poor description of the ^1D state at the one-determinant level.

(38) Moore, C. E. Atomic Energy Levels. *Nat. Stand. Ref. Data Ser., Nat. Bur. Stand. (U.S.)* **1971**, 35/V.

(39) Wiberg, K. B. *Tetrahedron* **1968**, *24*, 1083.

(40) The calculated small positive charge of the carbon atom in **1a** does not contradict the classification of the carbon ligand as a nucleophile. Carbon monoxide also reacts as a C-nucleophilic agent, although the carbon atom of CO carries a positive charge. The shape of the charge distribution has a stronger influence on the chemical reactivity than the atomic partial charge.

(41) Page 290 in ref 15.

(42) Cremer, D.; Kraka, E. *Angew. Chem.* **1984**, *96*, 612; *Angew. Chem., Int. Ed. Engl.* **1984**, *23*, 627.

(43) The complex **5** may also be considered as the final and yet unknown member of the series L_nFe-CX, where X = O, NR, CR_2, BR_3.

Table 4. Result of the NBO Analysis and Wiberg Bond Indices *P* at B3LYP/II

no.	formula	*P*(Fe−C)		occ	%Fe	4s(Fe)	4p(Fe)	3d(Fe)	2s(C)	2p(C)
1a	$(CO)_4Fe$-C(ax)	1.55	σ	1.98	65.77	2.65	0.13	97.22	14.42	85.16
			π	1.84	81.54	0.00	0.05	99.99	0.00	99.71
			π	1.84	81.54	0.00	0.05	99.99	0.00	99.71
2b	$(CO)_4Fe$-CH_2(eq)	0.93	σ	1.75	31.58	47.04	0.16	52.80	37.69	62.28
			π	1.84	68.26	0.00	0.28	99.72	0.00	99.99
3[a]	$I(CO)_3Fe$-CH	1.73	σ	1.85	38.24	16.81	9.27	73.92	53.44	46.49
			π	1.39	53.28	0.11	40.39	59.49	0.00	99.93
			π	1.48	57.40	0.34	28.64	71.02	0.00	99.93
4	$(CO)_4Fe$-CO(ax)	0.69	σ	1.90	29.92	42.03	0.16	57.81	63.73	36.27
5	$(CO)_4Fe$-$CBCl_3$	1.32	σ	1.90	44.71	26.22	0.10	73.68	39.84	60.09
			π	1.80	80.04	4.42	0.08	95.50	0.00	99.90
			π	1.69	78.78	13.27	0.19	86.54	0.00	99.90
		P(C−B)		occ	%C	2s(C)	2p(C)		2s(B)	2p(B)
		0.88	σ	1.98	68.45	60.07	39.88		23.51	76.32

[a] Keyword for three-center bond was used.

Table 5. Calculated Charge Distribution Given by the NBO Analysis at B3LYP/II[a]

			q			p(π)		
no.	[TM]	L	[TM]	Fe	C(L)	C(L)	[TM]→L(π)	[TM]←L(σ)
1a	$(CO)_4Fe$	C	−0.16	−0.49	0.16	0.47[b]	0.94	1.10
2b	$(CO)_4Fe$	CH_2	0.13	−0.42	−0.54	0.78	0.78	0.65
3	$I(CO)_3Fe$	CH	−0.16	−0.23	−0.05	0.74[b]	0.48	0.64
4	$(CO)_4Fe$	CO(ax)	−0.17	−0.54	0.59	2.16[b,c]	0.32	0.49
5	$(CO)_4Fe$	$CBCl_3$	0.24	−0.44	0.12	0.60[b]		

[a] Partial charge *q* and population of the p(π) AO of ligands. [b] Doubly degenerated orbital. The data give the occupation of a single orbital. [c] Occupation of the π orbital of CO.

that have more p character. Orbitals with higher s character are also energetically lower lying than those with more p character and, thus, lead to weaker donor−acceptor interactions. However, the strength of the metal−ligand interactions is mainly determined by the Fe→L π-back-donation. This will be discussed below.

Table 5 gives the charge distribution at the atoms and the orbital populations. The atomic partial charges indicate that the iron atom always carries a negative charge. The charge at Fe in **3** is smaller than in the other complexes. The ligands C, CH, and CO in **1a**, **3**, and **4** are positively charged and, thus, are net charge donor ligands, while CH_2 and $CBCl_3$ in **2b** and **5** are negatively charged (net acceptor ligands). It is noteworthy that the attachment of BCl_3 in **5** reverses the net charge flow from the $Fe(CO)_4$ metal fragment to the ligand. However, we want to point out that the total atomic charges are not a very useful probe for the interactions between the metal and the ligand, because they do not say anything about the topography of the charge distribution. A better probe for the charge distribution is the bond polarities shown in Table 4 and the orbital populations given in Table 5. The population of the p(π)-orbitals of the ligand atoms in the complex and in the free ligand and the partial charges make it possible to estimate the amount of Fe←L σ-donation and Fe→L π-back-donation.

The results in Table 5 show that the carbon ligand is the strongest σ-donor *and* the strongest π-acceptor of the four ligands. This explains the very short and strong Fe−C bond of **1a**. A surprising feature of **1a** is that it is energetically lower lying than **1b**. A qualitative discussion of the orbital interactions between a X_4TM fragment and a ligand L in a trigonal bipyramidal complex X_4TML led to the suggestion that strong π-acceptor ligands tend to occupy the equatorial site.[28] Yet, the strong π-accepting carbon ligand clearly prefers the axial position in $(CO)_4FeC$. We think that the preference for the axial position comes from the $(CO)_4Fe-C$ σ-interaction. Table 5 shows that the Fe←C σ-donation is even larger than the Fe→C π-back-donation. The discussion about the orbital interactions in X_4TM-L considered only the π-orbitals of L, but not the σ-orbitals.[28] Strong σ-donor ligands such as CN^- occupy the axial position in $(CO)_4FeCN^-$, which has been explained with the weak π-acceptor ability of the cyanide ligand.[28] We think that the preference for the axial or equatorial side is determined not only by the π-orbital interactions but also by the σ-orbitals. The latter effect is then responsible for the finding that **1a** is energetically lower lying than **1b**. The relative σ-donor/π-acceptor strength explains also why the equatorial form of the carbene complex **2b** is lower in energy than the axial form **2a**. Table 5 shows that the CH_2 ligand is a stronger π-acceptor than σ-donor, while the carbon ligand is a stronger σ-donor than π-acceptor.

The carbyne complex **3** has a still shorter Fe−L bond than **1a**, and the Wiberg bond index[39] (Table 4) for the Fe−CH bond is higher (1.73) than for the Fe−C bond (1.55). However, the CH ligand has already one p(π)-electron in the reference state of the neutral ligand, while carbon (^{1}D) has none. The Fe−CH π-bonds of **3** are less polarized toward the iron end than the π-bonds of **1a** (Table 4), but one of the four π-electrons of the former bonds comes from the ligand, while all four π-electrons of the Fe−C bond of **1a** come from Fe. Thus, the neutral CH ligand is actually a weaker π-acceptor than C and CH_2 (Table 5). The bonding situation of the neutral carbyne ligand in **3** is not directly comparable to the ligands in the carbon complex **1a** and the carbene complex **2b** because of the unpaired p(π)-electron of CH. The very short Fe−CH bond of **3** is caused by the large s character of the carbon σ-donor orbital (Table 4). The main conclusion from the NBO analysis is that the

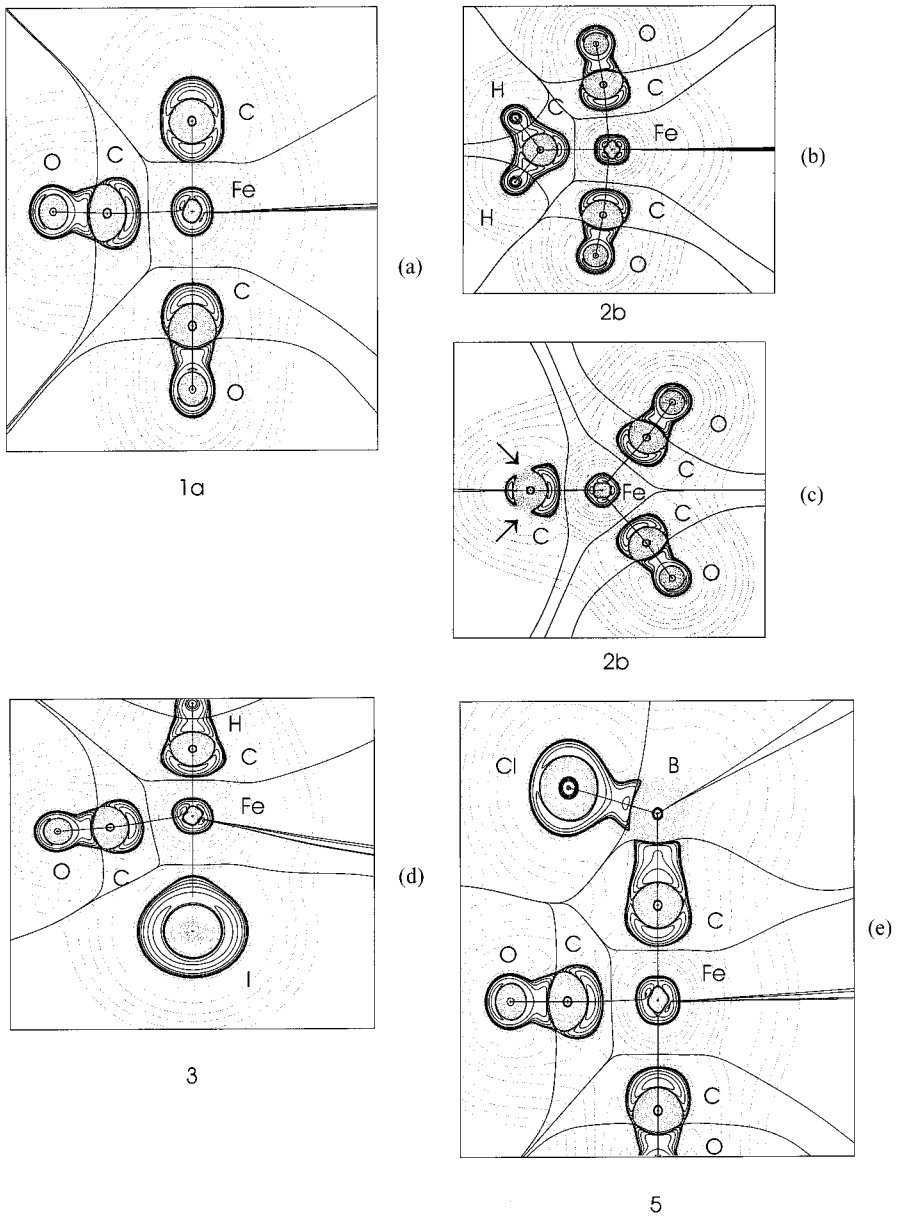

Figure 2. Contour line diagrams of the Laplacian distribution $\nabla^2\rho(\mathbf{r})$ at B3LYP/II. Dashed lines indicate charge depletion ($\nabla^2\rho(\mathbf{r}) > 0$); solid lines indicate charge concentration ($\nabla^2\rho(\mathbf{r}) < 0$). The solid lines connecting the atomic nuclei are the bond paths; solid lines separating the atomic nuclei indicate the zero-flux surfaces in the plane. The crossing points of the bond paths and zero-flux surfaces are the bond critical points $\mathbf{r}_b$. The arrows in (c) show the hole in the valence sphere of the carbene ligand that is prone to attack by a nucleophilic agent.

carbon ligand is a strong π-acceptor and an even stronger σ-donor.

The NBO results of **1** and **5** show that the p(π)-population of the carbon ligand atom is enhanced by the complexation with BCl_3. The population of the p(π) AOs of carbon in **5** is 1.20 e (0.60 e in each orbital), which is a significantly higher value than in the parent complex **1a** (0.94 e). Since the BCl_3 moiety induces a charge flow from $Fe(CO)_4$ to the $CBCl_3$ ligand, it may be argued that there is a stronger Fe→C π-back-donation in **5** than in **1a**. However, a part of the carbon p(π)-population of **5** may also be due to hyperconjugation from the BCl_3 ligand. The most important conclusion is that the carbon ligand atom in **5** becomes electronically stabilized and sterically shielded by the BCl_3 moiety.

The hybridization at the carbon donor atom of **5** explains why the C−BCl_3 bond is shorter yet weaker than the C−BCl_3 bond of $(NH_2)_2C$−BCl_3. Table 4 shows that the bond orbital of the C−BCl_3 bond has 60.1% s and 39.9% p character at the carbon side, while it has a much higher p character in the carbene complex (25.5% s, 74.3% p).[31] The more diffuse and energetically higher lying p-orbital induces stronger bonding at a larger distance. The $(CO)_4Fe$−C σ-bond of **5** is now more polarized toward the carbon end, while in **1a** it was more polarized toward Fe.

We carried out topological analyses of the electron density distribution of **1a**−**5** in order to seek further information about the electronic structure of the molecules. Figure 2a shows the contour line diagram of the Laplacian distribution $\nabla^2\rho(\mathbf{r})$ of **1a** in the plane that contains the carbon ligand atom. The most important finding is the continuous area of charge concentration ($\nabla^2\rho(\mathbf{r}) < 0$, solid lines) that is found around the carbon

Table 6. Results of the Topological Analysis of the Electron Density Distribution of $(CO)_4FeC$ (1a), $(CO)_4FeCH_2$ (2b), $I(CO)_3FeCH$ (3), $Fe(CO)_5$ (4), and $(CO)_4FeCBCl_3$ (5)[a]

molecule	no.	bond X−Y	$\rho(\mathbf{r}_b)$ [1/Å^3]	H_b [au/Å^3]	$R(X-\mathbf{r}_b)$ [Å]	$R(\mathbf{r}_b-Y)$ [Å]	$\nabla^2\rho(\mathbf{r}_b)$ [1/Å^5]
$(CO)_4FeC$	**1a**	Fe−C	1.778	−1.726	0.881	0.733	−1.358
		Fe−C(ax)	0.525	−0.116	1.010	1.042	8.513
		Fe−C(eq)	0.963	−0.506	0.940	0.879	10.064
		C−O(ax)	3.153	−5.159	0.377	0.763	32.337
		C−O(eq)	3.092	−5.064	0.380	0.768	29.270
$(CO)_4FeCH_2$	**2b**	Fe−C	1.032	−0.587	0.955	0.871	5.610
		C−H	1.850	−1.829	0.703	0.392	−22.743
		Fe−C(ax)	0.946	−0.493	0.909	0.902	11.031
		Fe−C(eq)	0.967	−0.515	0.921	0.885	10.593
		C−O(ax)	3.096	−5.081	0.380	0.768	28.663
		C−O(eq)	3.080	−5.044	0.381	0.769	28.539
$I(CO)_3FeCH$	**3**	Fe−C	1.628	−1.404	0.852	0.749	8.947
		C−H	1.854	−1.894	0.725	0.368	−24.912
		Fe−C(eq)	0.969	−0.512	0.935	0.885	9.472
		C−O(eq)	3.106	−5.091	0.379	0.767	29.966
		Fe−I	0.276	−0.027	1.183	1.588	1.821
$Fe(CO)_5$	**4**	Fe−C(ax)	0.907	−0.448	0.900	0.919	11.508
		Fe−C(eq)	0.989	−0.517	0.933	0.872	10.332
		C−O(ax)	3.100	−5.089	0.380	0.767	29.031
		C−O(eq)	3.071	−5.026	0.381	0.770	28.349
$(CO)_4FeCBCl_3$	**5**	Fe−C(B)	1.506	−1.211	0.861	0.792	7.940
		C−B	1.085	−0.991	1.087	0.500	3.802
		Fe−C(ax)	0.716	−0.274	0.947	0.974	9.718
		Fe−C(eq)	0.965	−0.508	0.941	0.880	9.596
		C−O(ax)	3.155	−5.178	0.377	0.763	32.146
		C−O(eq)	3.125	−5.126	0.379	0.765	31.024
		B−Cl	0.855	−0.801	0.563	1.288	−2.629

[a] $\rho(r_b)$, H_b, $\nabla^2\rho$ (r_b) are the electron density, the energy density, Laplacian at the bond critical point r_b, respectively. $R(X-\mathbf{r}_b)$ and $R(\mathbf{r}_b-Y)$ give the distance between the bond critical point $\mathbf{r}_b$ and the X or Y atom.

ligand. This is in strong contrast to the shape of the Laplacian distribution of the carbene carbon atom of **2a**, which is displayed in Figures 2b and 2c. The contour line diagram shown in Figure 2c exhibits the Laplacian distribution in the molecular plane that is perpendicular to the plane of the CH_2 ligand. There is clearly a "hole" in the area of charge concentration, which is indicated by the arrows. The charge depletion ($\nabla^2\rho(\mathbf{r}) > 0$, broken lines) at the carbene ligand of **2b** is directed toward the in-plane p(π)-orbital of the carbon atom. It shows the local electron deficiency at the carbene carbon atom, and it indicates the preferred direction for a nucleophilic attack.

The shape of the Laplacian distribution around the carbon ligand in **1a** (Figure 2a) is similar to that of the carbyne ligand in **3** (Figure 2d). The difference between the two ligands is that the carbon ligand of **1a** has an area of charge concentration pointing away from the metal, while the CH ligand of **3** has a bonded hydrogen atom. The large area of charge concentration at the carbon ligand pointing away from Fe suggests a possibly nucleophilic behavior of **1a** in chemical reactions.[40] The nucleophilicity of **3** comes to the fore by the strong attraction of the BCl_3 moiety in **5**. The Laplacian distribution of **5** is shown in Figure 2e. The shapes of the Laplacian distribution around the carbon atom of the $CBCl_3$ ligand of **5** and the carbon atom of the CH ligand of **3** are very similar. Thus, the bond energy calculations, the topological analysis of the electron density distribution, and the NBO calculations suggest that **5** might perhaps become isolated under appropriate conditions.

Table 6 gives the numerical results of the topological analysis of the electron density distribution. The data support the suggestion that the iron−carbon bonds of **1a** and **5** have a significant covalent character. It has been shown that typical covalent bonds have large charge densities at the bond critical point ρ_b[41] and that the energy densities at the bond critical point H_b is negative and large in magnitude.[42] Table 6 shows that the Fe−C bonds of **1a** and **5** have strongly negative H_b values and large positive ρ_b values.

Summary and Conclusion

The results of this study can be summarized as follows. The carbon complex $(CO)_4FeC$ (**1a**) is a minimum on the singlet potential energy surface. Structure **1a** possesses an axial Fe−C bond, which has a theoretically predicted large dissociation energy, $D_e = 84.1$ kcal/mol at B3LYP/II and $D_e = 94.5$ kcal/mol at CCSD(T)/II. The carbon ligand is a strong π-acceptor and an even stronger σ-donor. The analysis of the electronic structure of **1a** suggests that the carbon ligand atom should behave like a nucleophile. The donor−acceptor complex $(CO)_4FeC-BCl_3$ (**5**) has a calculated C−B bond energy of $D_e = 25.6$ kcal/mol at B3LYP/II and might become isolated under appropriate conditions.

Acknowledgment. This work was supported by the Deutsche Forschungsgemeinschaft and by the Fonds der Chemischen Industrie. Excellent service by the HRZ Marburg is gratefully acknowledged. Additional computer time was given by the HLRZ Stuttgart and the HHLR Darmstadt.

Supporting Information Available: Table containing the calculated vibrational spectra of **2**−**4**. This material is available free of charge via the Internet at http://pubs.acs.org.

OM000250O